Resonance phenomena in the region of overlap between NMR and ESR

V. A. Ignatchenko and V. P. Tsifrinovich

L. V. Kirenskiĭ Institute of Physics, Siberian Branch of the Academy of Sciences of the USSR, Krasnoyarsk
Usp. Fiz. Nauk **133**, 75–102 (January 1981)

A review is given of theoretical and experimental research in the new field of magnetic resonance in the case of overlap between nuclear and electron spin resonance frequencies in magnetically ordered media. Particular attention is devoted to the typical (for magnetic materials) situation in which the electron relaxation parameter is much greater than the dynamic electron-nuclear interaction parameter. Both stationary and transient phenomena are considered. Recently discovered new effects in the overlap region are examined in detail. It is shown that NMR signals can be detected by simple ferro- and anti-ferromagnetic resonance methods.

PACS numbers: 76.30. – v, 76.60. – k, 07.58. + g

CONTENTS

Introduction 42
1. Equations of motion and basic features of the electron-nuclear magnetic system 42
2. Natural frequencies and damping of electron-nuclear oscillations 44
   A. Natural frequencies of interacting oscillators 44
   B. Electron-nuclear magnetic oscillations 45
   C. Electron-nuclear spin waves 46
3. Susceptibility of the system 47
   A. Coupled oscillators 47
   B. Electron-nuclear magnetic resonance 48
   C. Shift of FMR 50
   D. Effect of inhomogeneities 50
   E. Experiment 52
4. Transient processes 53
   A. Nuclear-electron relaxation and spin echo 53
   B. ENMR in inverted state 54
   C. Experiment 55
Conclusions 55
References 56

INTRODUCTION

Recent years have seen rapid development of research into nuclear magnetic resonance in magnetically ordered materials. These studies have now assumed practical importance because of applications of nuclear spin echo in radioengineering. Under the usual experimental conditions, the electron spin resonance frequency is much higher than the frequency of nuclear magnetic resonance. Review papers published during the last decade have therefore been concerned with this situation. In the present review, on the other hand, we consider the new region in which the nuclear magnetic and electron spin resonance frequencies overlap. This overlap region represents, in a certain sense, the extremal state of the electron-nuclear magnetic system, and has long attracted the attention of theoreticians and experimenters. However, substantial progress has been achieved in this direction only in the last few years, and this has been responsible for the need for a new review.

We shall confine our attention to simplest magnetic structures, namely, uniformly magnetized ferromagnetic and antiferromagnetic materials. All fundamental questions will be discussed by considering the example of an isotropic ferromagnetic sphere, and some particular expressions will be given for uniaxial ferromagnets and antiferromagnets with an "easy plane."

1. EQUATIONS OF MOTION AND BASIC FEATURES OF THE ELECTRON-NUCLEAR MAGNETIC SYSTEM

When the temperature is much less than the terromagnetic Curie temperature T_c, electron spins are ordered and nuclear spins are in the paramagnetic state. Accordingly, the equations of motion for the electron magnetization $\mathbf{M}$ and the nuclear magnetization μ are the Landau-Lifshitz and Bloch[2] equations:

$$\left.\begin{aligned} \dot{\mathbf{M}} &= -\gamma_e[\mathbf{M}\times\mathbf{H}^e] + \frac{\xi}{M}[\mathbf{M}\times\dot{\mathbf{M}}], \\ \dot{\mu} &= \gamma_n[\mu\times\mathbf{H}^n] - \frac{\mathbf{k}(\mu_z+\mu)}{T_1} - \frac{\mathbf{i}\mu_x+\mathbf{j}\mu_y}{T_2}, \\ \mathbf{H}^e &= -\frac{\delta\mathcal{H}}{\delta\mathbf{M}}, \quad \mathbf{H}^n = -\frac{\delta\mathcal{H}}{\delta\mu}, \end{aligned}\right\} \tag{1.1}$$

where ξ is the dimensionless parameter representing the damping of electron magnetization, and T_1 and T_2 are, respectively, the longitudinal and transverse relaxation times for nuclear magnetization. The electron gyromagnetic ratio is $\gamma_e > 0$ and the negative sign in front of γ_e is shown explicitly in the first equation; the nuclear gyromagnetic ratio γ_n can be both greater than or less than zero, but, for most magnetic materials, $\gamma_n > 0$.

The density of the phenomenological Hamiltonian $\mathcal{H}$ contains the hyperfine magnetic interaction term[3]

$$\mathcal{H}_1 = A\mu\cdot\mathbf{M}. \tag{1.2}$$

 0038-5670/81/010042-15$01.10

where $A \sim 100-1000$ is the dimensionless hyperfine interaction constant. This interaction gives rise to an additional effective magnetic field both in the nuclear and electron magnetic subsystems:

$$\mathbf{H}_1^n = -A\mathbf{M}, \quad \mathbf{H}_1^e = -A\boldsymbol{\mu}. \tag{1.3}$$

Whilst, in most cases, H_1^e is negligible in comparison with other fields acting on the electron magnetization (the constant external field, the magnetic anisotropy field, and the magnetic dipole field), the component H_1^n reaches values of the order of 10^5-10^6 Oe and, as a rule, is the main field governing the magnitude and orientation of nuclear magnetization. We shall therefore omit the subscript 1 in the field H^n and will assume that this field is entirely determined by $A\mathbf{M}\cdot\boldsymbol{\mu}$. The quantity μ is calculated as the magnetization of the paramagnetic system made up of the nuclear spins in the magnetic field $A\mathbf{M}$. The direction of the vector $\boldsymbol{\mu}$ in the ground state is opposite to the direction M, in accordance with the negative sign of H^n. We shall assume that, in the ground state, both the external magnetic field H and the electron magnetization M lie along the z axis. In Bloch's equation (1.1), therefore, we have taken the plus sign in the expression $(\mu_z + \mu)$, which describes longitudinal relaxation: the nuclear magnetization is in equilibrium when $\mu_z = -\mu$.

The considerable strength of the effective magnetic field at the nuclei, and the fact that it is proportional to the electron magnetization M, have a distinctive effect on the entire dynamics of nuclear magnetization in magnetically ordered media: they give rise to certain characteristic features in the motion of μ as compared with the dynamics of μ in materials without magnetic order. Under normal conditions, when the electron resonance frequency ω_e is much higher than the nuclear resonance frequency ω_n, the basic features of NMR in magnetic materials are well known and have been described in review papers and monographs.[3-8] Let us briefly recall them.

In the first approximation, the expressions for the NMR and FMR frequencies (for simplicity, we consider an isotropic ferromagnetic sphere) are as follows:

$$\omega_n \approx \gamma_n A M, \quad \omega_e \approx \gamma_e H. \tag{1.4}$$

Thus, whilst the FMR frequency ω_e is determined by the external magnetic field (as is the NMR frequency in para- and diamagnetic materials), the NMR frequency ω_n in ferromagnets is determined by the hyperfine field experienced by the nucleus and, for $T \ll T_c$, it is a characteristic of the given material (for example, for cobalt $\omega_n/2\pi \simeq 200$ MHz, whereas, for iron, $\omega_n/2\pi \simeq 50$ MHz).

The transverse components of the hyperfine field that appear under the influence of an external time-dependent magnetic field $\mathbf{h}(t)$ perpendicular to the Z axis give rise to a distinctive amplification effect. The field h produces transverse components of electron magnetization and, consequently, transverse components of the hyperfine field $\mathbf{h}^n$. The nuclear magnetization then experiences the resultant field $\mathbf{h}+\mathbf{h}^n$, but $\mathbf{h}^n$ is stronger than h by a factor of η, where η is the amplification coefficient[3]:

$$\eta = A\chi_0 = \frac{H^n}{H^k + H} \sim 10^2 - 10^4 \tag{1.5}$$

where χ_0 is the static transverse susceptibility of the electron magnetic system and H^k is the anisotropy field (we assume that the specimen is magnetized along the anisotropy axis). The nuclear magnetization is thus in an exceedingly strong hyperfine field $\mathbf{h}^n(t)$, and the radiofrequency field $\mathbf{h}(t)$ can be neglected in comparison with it. However, this does not exhaust the role of η. The response of the nuclear system, i.e., the appearance of the transverse components $\mu_\perp(t)$, induces a hyperfine field in the electron system which responds to it with the transverse component $\mathbf{m}_\perp(t)$. The apparatus records the resultant response $\mu_\perp + \mathbf{m}_\perp$, but $\mathbf{m}_\perp$ exceeds $\mu_\perp$ by a factor of η, and the direct response of the nuclear system can be neglected. Thus, the excitation and detection of the nuclear signal in the magnetically ordered medium occur through the electron magnetic system. Mathematically, this is represented by the fact that it is the square of the coefficient η that appears in the resultant response:

$$\mathbf{m}_\perp = \eta^2 \hat{\chi}_n \mathbf{h} \tag{1.6}$$

where $\hat{\chi}_n$ is the nuclear susceptibility tensor.

The dynamics of the electron-nuclear magnetic system can, in general, be described by five nonlinear first-order equations (three equations for the components of μ and two equations for the components of M, whose modulus is conserved). An essential simplification of this complicated problem is achieved by introducing the following two fundamental assumptions:

a) The electron magnetization is written in the form

$$\mathbf{M}(t) = \mathbf{k}M + \mathbf{m}(t), \quad |\mathbf{m}| \ll M, \tag{1.7}$$

so that (1.1) can be linearized in the transverse components of the electron magnetization m, whilst retaining the equation for the nuclear magnetization μ in its nonlinear form.

b) When the frequency ω is much less than the electron resonance frequency ω_e, we may use the quasistatic approximation for the Landau–Lifshitz equation

$$[\mathbf{M} \times \mathbf{H}^e] = 0. \tag{1.8}$$

When these approximations are adopted, the Landau–Lifshitz equation (1.8) yields the following simple expression for the transverse components of electron magnetization:

$$\mathbf{m} = \chi_0 (\mathbf{h} - A\boldsymbol{\mu}_\perp). \tag{1.9}$$

Substituting this in the second equation in (1.1), we obtain a set of three nonlinear first-order equations for the components of the nuclear magnetization μ. When the magnetic field h rotates with frequency ω in the xy plane of the coordinate frame attached to this field, the equations become[9]

$$\begin{aligned} &\dot{u} - \omega_n v + \frac{u}{T_2} + L_y = -\omega_y m, \\ &\dot{v} + \omega_n u + \frac{v}{T_2} + L_x = -\omega_x m, \\ &\dot{m} + \frac{(m-1)}{T_1} + L_z = -(\omega_y u + \omega_x v) \end{aligned} \tag{1.10}$$

where

$$u = \frac{\mu_x}{\mu}, \quad v = -\frac{\mu_y}{\mu}, \quad m = -\frac{\mu_z}{\mu}, \quad \omega_i = \gamma_n \eta h_i,$$
$$y = \omega_n - \omega, \quad L_y = Dmv, \quad L_x = -Dmu, \quad L_z = 0, \quad D = \gamma_n A^2 \chi_0 \mu.$$

The numerous results obtained in the theory of nuclear resonance in ferromagnets for $\omega_n \ll \omega_e$ are based on (1.10) or an equivalent set of equations corresponding to assumptions (1.7)–(1.8). Some of these results, i.e., those corresponding to the linear motion of nuclear magnetization ($\mu_z \simeq -\mu$), were given above. Other results include the dynamic shift of the NMR frequency,[3] which is described by the nonlinear terms L_i in (1.10). In the linear situation ($\mu_z \simeq -\mu$), the dynamic shift is a maximum: the NMR frequency is then decreased by the amount

$$D = \frac{\eta\omega_n\mu}{M} = \frac{\gamma_e A\mu\omega_n}{\omega_e}. \tag{1.11}$$

It is clear that the dynamic frequency shift increases with decreasing electron resonance frequency ω_e (however, $\mu_e \gg \omega_n$ must remain; the entire foregoing discussion becomes invalid when this condition is not satisfied). In the nonlinear situation, the dynamic frequency shift leads to many features of pulsed phenomena such as new mechanisms for the formation of nuclear spin echo, which have been extensively investigated both theoretically and experimentally in recent years.[6-8]

2. NATURAL FREQUENCIES AND DAMPING OF ELECTRON-NUCLEAR MAGNETIC OSCILLATIONS

It is clear from (1.4) that, as the magnetic field H decreases, the NMR and FMR frequencies approach one another and may even overlap, so that $\omega_e = \omega_n$. The approximation defined by (1.8) then becomes invalid and we must return to the complete system given by (1.1). In the linear approximation, to which we will confine our attention in this and the next sections, Eq. (1.1) consists of four coupled first-order equations for the transverse components of nuclear and electron magnetizations.[10] These equations describe a system of two interacting oscillators. In the special case of complete magnetic isotropy in the xy plane, the number of coupled equations can be reduced to two by introducing circular projections for the transverse components of μ and $\mathbf{M}$.

A. Natural frequencies of interacting oscillators

We recall the general properties of the natural frequencies of a set of two interacting oscillators by considering a simple example that can be described by first-order equations. The complex natural frequencies are then given by

$$(\omega_e - \omega + i\Gamma_e)(\omega_n - \omega + i\Gamma_n) - \frac{\omega_q^2}{4} = 0, \tag{2.1}$$

where ω_e and ω_n are the unperturbed resonance frequencies of the oscillators, Γ_e and Γ_n are their relaxation parameters, and ω_q is the oscillator interaction parameter.

Substituting $\omega = \omega' + i\omega''$, we obtain from (2.1) the following two equations for $x + y \neq 0$:

$$xy\left[1 + \left(\frac{\Gamma_e - \Gamma_n}{x+y}\right)^2\right] - \frac{\omega_{q'}^2}{4} = 0,$$
$$\omega'' = \frac{x\Gamma_n + y\Gamma_e}{x+y}, \tag{2.2}$$

where $x = \omega_e - \omega'$, $y = \omega_n - \omega'$. The equation $x + y = 0$ corresponds to $\omega_e = \omega_n$ and $|\Gamma_e - \Gamma_n| > \omega_q$, in which case, the solution is

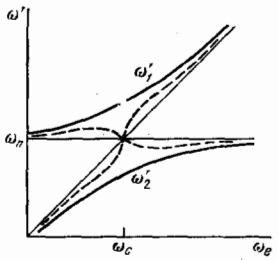

FIG. 1. Natural frequencies $\omega'_{1,2}$ of interacting oscillators. Solid curves correspond to $\omega_q > |\Gamma_e - \Gamma_n|$; broken curves correspond to the opposite inequality.

$$\omega'_{1,2} = \omega_e = \omega_n,$$
$$\omega''_{1,2} = \frac{1}{2}\left[(\Gamma_e + \Gamma_n) \pm \sqrt{(\Gamma_e - \Gamma_n)^2 - \omega_q^2}\right]. \tag{2.3}$$

The first equation in (2.2) describes the dependence of the real natural frequencies $\omega'_{1,2}$ on ω_e, which we shall vary by varying the separation between the unperturbed oscillator frequencies ω_e and ω_n. The solid curves in Fig. 1 show the solution in the absence of damping ($\Gamma_e = \Gamma_n = 0$). The intersecting straight lines represent the frequencies ω_n and ω_e of the unperturbed oscillators. The natural frequencies ω' are found to separate at $\omega_e = \omega_n = \omega_c$ by an amount equal to the interaction frequency ω_q. This effect corresponds to the separation of degenerate energy levels of a quantum-mechanical system when an interaction is introduced. As the distance from the point of intersection increases, the interaction effect becomes weaker and the natural frequencies tend to the corresponding unperturbed frequencies ω_e and ω_n. The foregoing discussion is also valid for damped oscillators if their relaxation parameters are equal, since the first equation in (2.2) involves only the modulus of the relaxation parameter difference $|\Gamma_e - \Gamma_n|$.

At the point ω_c, the frequency difference for $|\Gamma_e - \Gamma_n| < \omega_q$ is given by

$$(\omega'_1 - \omega'_2)_{\omega_e = \omega_c} = \sqrt{\omega_q^2 - (\Gamma_e - \Gamma_n)^2}. \tag{2.4}$$

As $|\Gamma_e - \Gamma_n|$ increases, the frequency difference decreases; the two frequencies become equal when $|\Gamma_e - \Gamma_n| > \omega_q$ (broken curves in Fig. 1). It is clear from the second equation in (2.2) that the damping of $\omega''_{1,2}$ at the point ω_c for $|\Gamma_e - \Gamma_n| < \omega_q$ is the same for the two branches, and is equal to the half-sum of the unperturbed damping parameters:

$$\omega''_{1,2}|_{\omega_e = \omega_c} = \frac{\Gamma_e + \Gamma_n}{2}. \tag{2.5}$$

When $|\Gamma_e - \Gamma_n| > \omega_q$, the damping at ω_c is described by (2.3). For $|\Gamma_e - \Gamma_n| \gg \omega_q$, Eq. (2.3) yields

$$\omega''_1 \approx \Gamma_e - \frac{\omega_q^2}{4|\Gamma_e - \Gamma_n|}, \quad \omega''_2 \approx \Gamma_n + \frac{\omega_q^2}{4|\Gamma_e - \Gamma_n|}. \tag{2.6}$$

As the distance from the crossing point increases, and independently of the relationship between $|\Gamma_e - \Gamma_n|$ and ω_q, the damping of each natural frequency tends to the unperturbed damping of the corresponding oscillator.

B. Electron-nuclear magnetic oscillations

Let us now consider the difference between the model system consisting of two simple oscillators and a real system of coupled NMR and FMR (AFMR). As noted above, in the special case of magnetic isotropy in the x, y plane, the introduction of circular projections gives rise to a considerable simplification of the problem. The complex electron-nuclear frequencies of magnetic oscillations corresponding to resonance projections μ^+ and m^+ are described by

$$(\omega_e - \omega + i\xi\omega)\left(\omega_n - \omega + \frac{i}{T_2}\right) - \gamma_e\gamma_n A^2\mu M = 0. \qquad (2.7)$$

It is clear that this situation is very close to the system of two simple oscillators (2.1). However, Eq. (2.7) has a new feature connected with the sign of the gyromagnetic ratio. The electron gyromagnetic ratio is $\gamma_e > 0$, i.e., we have introduced explicitly the negative sign in front of γ_e in the Landau-Lifshitz equation. On the other hand, γ_n can be either positive or negative. For $\gamma_n > 0$, the projections m^+ and μ^+ correspond to the resonance situation, whereas m^- and μ^- correspond to the nonresonance situation. For $\gamma_n < 0$, the resonance projections are m^+ and μ^-. The equations for the natural frequencies in this case have the form (damping is neglected for simplicity):

$$\begin{aligned} &\text{for } m^+,\ \mu^+\text{: } (\omega_e - \omega)(\omega_n + \omega) - \frac{\omega_q^2}{4} = 0, \\ &\text{for } m^-,\ \mu^-\text{; } (\omega_e + \omega)(\omega_n - \omega) - \frac{\omega_q^2}{4} = 0; \end{aligned} \qquad (2.8)$$

where $\omega_n = |\gamma_n| AM$, $\omega_q^2 = 4\gamma_e|\gamma_n|A^2M\mu$. There is no resonance interaction between the oscillators in this case: the degenerate levels do not split. The first equation describes the FMR frequency, modified by the interaction with the nonresonance projection μ^+, and the second gives the NMR frequency modified by the interaction with the nonresonance projection m^-:

$$\omega_1 \approx \omega_e - \frac{\omega_q^2}{4(\omega_e + \omega_n)}, \quad \omega_2 \approx \omega_n - \frac{\omega_q^2}{4(\omega_e + \omega_n)}. \qquad (2.9)$$

When $\omega_e = \omega_n$, these frequencies are equal. It is interesting to note that, when $\omega_n \ll \omega_e$, this situation is indistinguishable from the case $\gamma_n > 0$. It is clear from (2.9) that the dynamic frequency shift has the same sign and is given by the same equation (1.11). Moreover, the absence of splitting of oscillations with opposite polarization is of purely academic interest in this case, since $\gamma_n > 0$ for the nuclei of all the main magnetically ordered materials. In addition, for $\gamma_n < 0$, the situation described by (2.8) will be observed only for complete magnetic isotropy in the x, y plane. Magnetic crystallographic anisotropy in this plane or shape anisotropy lead to the coupling between the right and left polarized components of electron magnetization m^+ and m^- and, consequently, to the resonance interaction between the electron and nuclear magnetic oscillators for any sign of γ_n.

The basic question, i.e., whether it is physically possible to reduce ω_e down to ω_n, is intimately connected with shape anistropy and magnetic crystallographic anisotropy. For a magnetic ellipsoid with arbitrary ratio of semiaxes, the FMR frequency is given by

$$\omega_e = \sqrt{\omega_x\omega_y},$$

where

$$\begin{aligned} \omega_x &= \gamma_e[H + H_1 + (N_x - N_z)M + H_\Delta], \\ \omega_y &= \gamma_e[H + H_2 + (N_y - N_z)M + H_\Delta]; \end{aligned} \qquad (2.10)$$

in which $H_\Delta = A\mu, N_i$ are the demagnetizing factors for the ellipsoid, and H_1, H_2 are determined by the magnetic anisotropy. For example, in the case of uniaxial anisotropy along the z axis, we have $H_1 = H_2 = H^k$. On the other hand, if the anisotropy is along the x axis, $H_1 = -H^k, H_2 = 0$.

We shall now consider the effect of the shape of the specimen, neglecting for the moment the static interaction with the nuclear system H_Δ and anisotropy. To ensure that the specimen is magnetized uniformly by the magnetic field in the Z direction, it is necessary (but not always sufficient) for the internal field in the specimen $H_i = H - N_z M$ to be greater than zero. This yields the necessary condition[10] for the point $\omega_e = \omega_n$ to be reached:

$$\gamma_n A > \gamma_e\sqrt{N_x N_y}. \qquad (2.11)$$

In practice, this means that the point at which the two frequencies ω_e and ω_n become equal may lie in the physical domain only for specimens for which one or both demagnetizing factors in the xy plane are close to zero. Specimens of this kind include: (a) a thin plate magnetized either in its plane or at right-angles to it, and (b) a long cylinder magnetized at right-angles to its axis. Naturally, condition (2.11) may turn out to be insufficient in many cases: the additional condition is that the anisotropy field must be small or the situation must be such that this field can be compensated by an external field; the gap ω_Δ due to the static hyperfine field $H_\Delta = A\mu$ cannot be removed. The gap ω_Δ is very small in ferromagnets, but it may become appreciable in antiferromagnets because of the appearance of the exchange field H_E in the relevant expressions. For example, in "easy plane" ferromagnets, the frequency corresponding to the low-frequency branch of AFMR and the size of the gap are given by

$$\omega_e = \gamma_e\sqrt{\alpha_e H + H_\Delta}\sqrt{H_E}, \quad \omega_\Delta = \gamma_e\sqrt{H_\Delta H_E}, \qquad (2.12)$$

where $\alpha_e = (H + H_D)/H_E$ is the angle between the sublattices, H_D is the Dzyaloshinskiĭ field, $H_E = 2JM$ is the exchange field, and J is the exchange integral.

The natural frequencies of electron-nuclear magnetic oscillations in the region where ω_e and ω_n overlap were initially investigated without taking damping into account.[11-12] In the general case of a ferromagnet, they are described by

$$(\omega^2 - \omega_e^2)(\omega^2 - \omega_n^2) - \gamma_e\gamma_n A^2 M\mu(2\omega^2 + \omega_n\omega_x + \omega_n\omega_y - \gamma_e\gamma_n A^2 M\mu) = 0. \qquad (2.13)$$

When $\omega_n \ll \omega_e$, this equation shows that the maximum dynamic NMR frequency shift is

$$D = \gamma_e\gamma_n A^2 M\mu\frac{\omega_x + \omega_y}{2\omega_e^2}. \qquad (2.14)$$

At $\omega_e = \omega_n$, the difference between the natural frequencies is determined by the dynamic electron-nuclear interaction parameter ω_q. For a ferromagnet,

$$\omega_q^2 = \gamma_e\gamma_n A^2 M\mu\left(1 + \frac{\omega_x}{\omega_n}\right)\left(1 + \frac{\omega_y}{\omega_n}\right). \qquad (2.15)$$

The magnitude of ω_q depends on the shape of the specimen. This dependence or, more precisely, the dependence on the degree of ellipticity of the locus of M, is connected with the fact that the dynamic electron-nuclear coupling will be stronger as the electron susceptibility χ_e increases. The expressions for ω_x and ω_y given by (2.10) can be rewritten in the form

$$\omega_x = \frac{\gamma_e M}{\chi_{0x}}, \quad \omega_y = \frac{\gamma_e M}{\chi_{0y}}, \tag{2.16}$$

where χ_{0x}, χ_{0y} are the static susceptibilities of the electron system along the x and y axes, respectively. The condition $\omega_e = \omega_n$ defines the product $\chi_{0x}\chi_{0y}$. Therefore, to increase the susceptibility along one of the axes (for example, the x axis), we must simultaneously reduce the susceptibility along the other axis (the y axis). The result will be that ω_q will reach its maximum value in the case of maximum asymmetry in the precession plane, i.e., $\omega_y/\omega_x \gg 1$. When this is so, we have the following expressions for ferro- and antiferromagnets:

$$\omega_q \approx \sqrt{\gamma_e A \mu \omega_y}, \quad \omega_q \approx \gamma_e \sqrt{A \mu H_E} \tag{2.17}$$

respectively. For the remainder of this section, we shall write all our mathematical expressions for the case of strong asymmetry, for which electron susceptibility is a maximum along the x axis: $\chi_{0y} \ll \chi_{0x} = \chi_0$. In easy-plane antiferromagnets, the ellipticity of the locus of magnetization of a sublattice is stronger than in ferromagnets. In ferromagnets, therefore, the magnitude of ω_q will be much greater than in ferromagnets. Finally, we note that the expressions given by (2.17) for ferro- and antiferromagnets are the same as the corresponding expressions for the hyperfine gap ω_Δ in the spectrum of unperturbed electron resonance. This is so because the static and dynamic hyperfine interactions are determined by the same scalar quantity, namely, A.

The effect of relaxation on the natural frequencies of electron-nuclear oscillations was first examined by Portis[13] and later, and in greater detail, by Ignatchenko and Tsifrinovich.[14] As already noted, the behavior of the natural frequencies is wholly determined by the relationship between $|\Gamma_e - \Gamma_n|$ and ω_q. In magnetically ordered media, we usually have $\Gamma_n \ll \Gamma_e$ and the behavior of the natural frequencies is determined by the relationship between ω_q and Γ_e. When $\omega_q \gg \Gamma_e$, the overlap region contains two equivalent modes of coupled electron-nuclear oscillations with complex frequencies $\tilde{\omega}_{1,2}$. At $\omega_e = \omega_n$, we have

$$\omega_{1,2} \approx \omega_n \pm \frac{1}{2}\sqrt{\omega_q^2 - \Gamma_e^2} + \frac{i\Gamma_e}{2}, \quad \Gamma_e \approx \frac{\xi\omega_y}{2}. \tag{2.18}$$

When $\omega_q \ll \Gamma_e$, the natural oscillations in the overlap region can be reliably separated into electron-like oscillations with frequency $\tilde{\omega}_e$ and nuclear-like with frequency $\tilde{\omega}_n$. To within terms $\sim\mu$, we then have[15]

$$\tilde{\omega}_n(H) = (\omega_n - D) + i(\Gamma_n + \Gamma_\varkappa), \quad D = \gamma_n A^2 \chi_e'(H)\mu, \quad \Gamma_\varkappa = \gamma_n A^2 \chi_e''(H)\mu, \quad \Gamma_n = \frac{1}{T_2}, \tag{2.19}$$

where $\chi_e'(H)$ and $\chi_e''(H)$ are the real and imaginary parts of the electron susceptibility at the NMR frequency, respectively:

$$\chi_e = \chi_0 \frac{\omega_e^2}{2\Gamma_e\omega} \frac{t-i}{t^2+1}, \quad t = \frac{\omega_e^2 - \omega^2}{2\Gamma_e\omega}. \tag{2.20}$$

These expressions are valid for ferromagnets. In the case of antiferromagnets, we must distinguish the susceptibility of the specimen χ_e from that of the sublattice $\chi_{e\nu}$. Since the nuclear magnetization of the sublattice interacts with the electron magnetization of only its own sublattice, we can replace χ_e with $\chi_{e\nu}$ in the expressions for D and $\Gamma_\varkappa$. In easy-plane antiferromagnets, $\chi_{e\nu} = \chi_e/\alpha_e$, where α_e is defined above.

It is clear from (2.19) that the dynamic shift of the frequency of nuclear oscillations D is determined by the real part of the electron susceptibility $\chi_e'(H)$. The magnitude of D is a maximum for $\omega_e(H) = \sqrt{\omega_n^2 + 2\Gamma_e\omega_n}$ and vanishes at the overlap point $\omega_e = \omega_n$. The damping coefficient of nuclear-like oscillations increases the amount $\Gamma_\varkappa$, which is the parameter of the nuclear-electron relaxation (NER), i.e., relaxation in the nuclear system due to the damping of electron magnetization. The parameter $\Gamma_\varkappa$ is determined by the imaginary part of the electron susceptibility, $\chi_e''(H)$, and reaches its maximum at the frequency overlap point. The maximum values of D and $\Gamma_\varkappa$ are determined to within a factor of 0.5 by the same parameter $\omega_q^2/4\Gamma_e$. It is clear that the magnitude of $\omega_q^2/4\Gamma_e$ is the renormalized parameter of the dynamic electron-nuclear interaction in the case of strong relaxation of the electron magnetization.

We note that, whatever the relationship between Γ_e, Γ_n, and ω_q, the electron-nuclear oscillation frequencies are related by

$$|\tilde{\omega}_1\tilde{\omega}_2| = \omega_e^0(H)\omega_n, \quad \omega_1'' + \omega_2'' = \Gamma_e + \Gamma_n, \tag{2.21}$$

where $\omega_e^0 = \sqrt{\omega_e^2 - \omega_q^2}$ is the frequency of the electron resonance in the absence of the nuclear system.

C. Electron-nuclear spin waves

We shall now briefly consider electron-nuclear spin waves in the overlap region. Analysis on the basis of the equations of motion[12,15,16] has shown that, in the absence of relaxation, the curves representing ω' as a function of the wave vector k will separate in the overlap region. An analogous result follows also from quantum theory.[17-19]

When electron relaxation is large enough, the natural frequencies will cross, just as in the case of uniform oscillations, and the coupled oscillations can be unambiguously separated into electron-like and nuclear-like spin waves.[15] For a uniaxial ferromagnet, for example, the complex electron-like spin-wave frequency is given by the following expression to within terms of the order of $\sim\mu$:

$$\tilde{\omega}_{ek} = \omega_{ek}\left(1 + d_{ek}^4 \frac{\omega_{ek}^2 - \omega_n^2}{2\omega_{ek}^2 B_k^4}\right) + i\Gamma_{ek}\left(1 - \frac{d_{ek}^4}{B_k^4}\right), \tag{2.22}$$

and the complex frequency of the nuclear-like spin wave is given by

$$\tilde{\omega}_{nk} = \omega_n\left(1 + d_{nk}^4 \frac{\omega_n^2 - \omega_{ek}^2}{2\omega_n^2 B_k^4}\right) + i(\Gamma_n + \Gamma_{\varkappa k}), \quad \Gamma_{\varkappa k} = \frac{\Gamma_{ek} d_{nk}^4}{B_k^4}; \tag{2.23}$$

where ω_{ek} and Γ_{ek} are the frequency and damping parameter of the electron spin waves[20]

$$\omega_{ek} = \sqrt{\Omega_1\Omega_2 + 4\pi\gamma_e M(\Omega_1 \sin^2\varphi_k + \Omega_2 \cos^2\varphi_k)\sin^2\theta_k},$$
$$\Omega_1 = \gamma_e(H + A\mu + H_1 + \alpha M k^2 - N_z M),$$
$$\Omega_2 = \gamma_e(H + A\mu + H_2 + \alpha M k^2 - N_z M), \qquad (2.24)$$
$$\Gamma_{ek} = \frac{\xi\sigma_k}{2}, \quad \sigma_k = \Omega_1 + \Omega_2 + 4\pi\gamma_e M \sin^2\theta_k,$$

θ_k and φ_k are the polar and azimuthal angles of the wave vector k, respectively, and

$$d_{ek}^1 = 2\gamma_e A\mu\omega_n(\omega_{ek}^2 + \sigma_k\omega_n), \qquad (2.25)$$
$$d_{nk}^1 = 2\gamma_e A\mu\omega_n^2(\omega_n + \sigma_k), \quad B_k^1 = (\omega_{ek}^2 - \omega_n^2)^2 + 4\Gamma_{ek}^2\omega_n^2.$$

The expressions given by (2.22)–(2.25) show that the electron spin wave with wave vector k will, in a way, "generate" a nuclear spin wave with the same wave vector. These expressions are valid if the relaxation parameter of the electron spin wave, Γ_{ek}, is much greater than the dynamic interaction parameter ω_{qk} between the corresponding wave and the nuclear system:

$$\omega_{qk} = \sqrt{2\gamma_e A\mu(\omega_n + \sigma_k)}. \qquad (2.26)$$

If the dispersion curves for the electron spin waves (for fixed θ_k and φ_k) cross the NMR frequency ω_n, the order of magnitude of the maximum shift of the natural frequencies ω_k' and damping coefficients ω_k'' is determined by the renormalized dynamic interaction parameter $\omega_{qk}^2/4\Gamma_{ek}$. Hence, it follows that the width of the dispersion band for the nuclear-like spin waves is of the same order as their damping coefficients.

We recall that the electron resonance frequency ω_e is not necessarily equal to the minimum frequency ω_{ek}^{min} of the electron spin waves. In general, if the electron resonance frequency ω_e is equal to the NMR frequency, the frequencies of a whole group of electron spin waves will also be equal to the NMR frequency. Moreover, the geometry of the experiment can be chosen so that the electron spin wave frequencies ω_{ek} will cross the NMR frequency ω_n even in sufficiently strong fields when $\omega_e \gg \omega_n$. For example, for a thin plate magnetized in its own plane, we have $N_z = 0$ and, consequently, $\omega_{ek}^{min} \ll \omega_e$. We shall return to this situation in Sec. 4.

3. SUSCEPTIBILITY OF THE SYSTEM

A. Coupled oscillators

Let us now consider the behavior of a set of two interacting oscillators—nuclear and electron—under the influence of an external force, i.e., the time-dependent magnetic field h(t). This force acts on both oscillators but, because of the amplifying properties of the hyperfine interaction, its direct effect on the nuclear oscillator can be neglected: this oscillator is excited mainly through the coupling with the electron oscillator. This is also valid for the response: the direct response of the nuclear oscillator is much weaker than the response through the coupling between the oscillators. A close analog of a system of interacting FMR and NMR will therefore be two coupled oscillatory circuits ("e" and "n"), of which only one ("e") plays an active role: it is connected to an external source and it is the current in this circuit that is measured. The experimenter should be able to use these measurements to extract data both on the circuit which he is using (FMR) and the circuit coupled to it (NMR).

The general properties of a system of two coupled circuits are well known (see, for example, Ref. 21). This system is widely used in radioengineering as a band-pass filter, wave trap, and so on. However, we are interested in its properties from a specific point of view, namely: what information about the system can be extracted from the readings of an instrument connected in the "e" circuit? We recall some of the general properties of the system by considering the simple example of NMR and FMR in a magnetically isotropic sphere. The complex susceptibility of the resonance component of electron magnetization is, in this case, given by

$$\chi = \frac{m^+}{h} \approx \frac{i\gamma_e M(\omega_n - \omega + i\Gamma_n)}{(\omega_e - \omega + i\Gamma_e)(\omega_n - \omega + i\Gamma_n) - (\omega_q^2/4)}. \qquad (3.1)$$

The absorption of the energy of the high-frequency field h(t) is proportional to the imaginary part of the susceptibility:

$$\chi'' = \gamma_e M \frac{\Gamma_e y^2 + \Gamma_n q^2}{(xy - q^2) + (\Gamma_e y + \Gamma_n x)^2},$$
$$x = \omega_e - \omega, \quad y = \omega_n - \omega, \quad q^2 = \frac{1}{4}\omega_q^2 + \Gamma_e\Gamma_n. \qquad (3.2)$$

In the first instance, we shall be interested in the point of overlap between the unperturbed oscillator frequencies ($\omega_e = \omega_n = \omega_c$) at which the interaction is a maximum. The form of the function $\chi''(\omega)$ is then determined by the relationship between the three parameters Γ_e, Γ_n, and ω_q; it is well known that $\chi''(\omega)$ will, in general, have either three extrema (minimum at $\omega = \omega_c$ and two side maxima) or one maximum at the point $\omega = \omega_c$. We recall that, when $\omega_q > |\Gamma_e - \Gamma_n|$, the natural frequencies will split and the damping coefficients will coincide. Two resonance frequencies will exist in this case, namely, ω_1' and ω_2', and the corresponding two resonance peaks will be well resolved if the separation between ω_1' and ω_2' is much greater than the damping of the two oscillators. For oscillators with similar linewidths

$$|\Gamma_e - \Gamma_n| \ll \Gamma_n, \quad |\Gamma_e - \Gamma_n| < \omega_q, \qquad (3.3)$$

the expression given by (3.2) with $x = y$ can be approximately written in the form

$$\chi'' \approx \frac{1}{2}\gamma_e M\Gamma_e\left[\frac{1}{(y-a)^2 + b^2} + \frac{1}{(y+a)^2 + b^2}\right],$$
$$a = \frac{1}{2}\sqrt{\omega_q^2 - (\Gamma_e - \Gamma_n)^2}, \quad b = \frac{\Gamma_e + \Gamma_n}{2}. \qquad (3.4)$$

Hence, it is clear that there are two identical resonances, in each of which the properties of the interacting oscillators have been averaged out. The positions of the resonance maxima and their widths correspond to the natural frequencies (2.4) and damping parameters (2.5). The resonances approach one another as ω_q decreases and, when ω_q is less than the critical value, they merge into a single resonance (Fig. 2). The two resonances can be resolved (in the absence of noise) provided

$$\omega_q > \omega_q^c = \sqrt{\frac{4\Gamma_n^3}{\Gamma_e + 2\Gamma_n}}. \qquad (3.5)$$

Resonance circuits with coupling just stronger than the critical value (curve 2 in Fig. 2) are used as band-pass

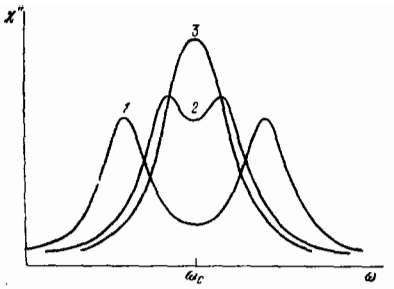

FIG. 2. Susceptibility (in relative units) of a system of two oscillators with $\omega_c > |\Gamma_q - \Gamma_n|$ when the coupling coefficient is greater than (1), close to (2), and less than (3) the critical value.

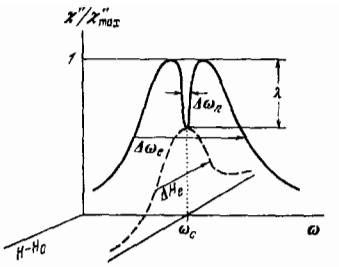

FIG. 3. Electron-nuclear magnetic resonance (ENMR) along the frequency axis (solid curve) and along the magnetic field axis (broken curve).

filters in radioengineering.

The first theoretical paper[22] devoted to the shape of the absorption lines in the NMR-FMR overlap region and based on the method of temperature Green's functions, was used to analyze the situation where there was very strong inhomogeneous broadening of the unperturbed NMR line: $\Gamma_3 \gg \Gamma_e$, where Γ_3 is the half-width of the NMR line due to the inhomogeneity of A. Two cases were considered, namely, $\omega_q \ll \Gamma_3$ and $\omega_q \gg \Gamma_3$. It was shown that, in the former case, the absorption line had only one maximum (corresponding to weak coupling in oscillator theory), whilst, in the latter case, there were two comparable and well-resolved maxima (corresponding to strong coupling). Moreover, a weak third maximum might occur[22] between these two strong maxima. This, in fact, takes us outside the framework of the theory of oscillators with a homogeneous absorption line, and depends on the shape of the distribution function for the hyperfine interaction constant, $f(A)$, over which the results reported in Ref. 22 were averaged. The third maximum vanishes when $f(A)$ is the Lorentz function.

Subsequently, a detailed analysis was carried out[23-25] of the situation characteristic for magnetic materials, within the framework of the Landau-Lifshitz and Block equations. This is characterized by the electron relaxation being much greater than the nuclear relaxation, i.e., $\Gamma_e \gg \Gamma_n, \Gamma_3$. Henceforth, we shall confine our attention to this particular situation.

B. Electron-nuclear magnetic resonance

Suppose that

$$\frac{4\Gamma_n^3}{\Gamma_e+2\Gamma_n} < \omega_q^2 < (\Gamma_e-\Gamma_n)^2. \tag{3.6}$$

When the right-hand side inequality is satisfied, the natural frequencies of the two interacting oscillators are equal at ω_c ($\omega_1' = \omega_2' = \omega_c$) and the two resonance peaks should coincide. On the other hand, when the left-hand inequality is satisfied, the function $\chi''(\omega)$ must have two maxima either side of ω_c and a minimum at ω_c. At first sight, this seems contradictory.

The parameters of magnetic materials typically obey a more stringent condition than is indicated by (3.6), i.e.,

$$\Gamma_e \gg \Gamma_n, \ \omega_q. \tag{3.7}$$

The expression for the imaginary part of the susceptibility of the system can then be approximately represented by the product of two factors

$$\chi'' \approx \frac{\gamma_e M \Gamma_e}{x^2+(\Gamma_e-p)^2} \frac{x^2+\Gamma_n(\Gamma_n+p)}{x^2+(\Gamma_n+p)^2}, \tag{3.8}$$

where $p = \omega_q^2/4\Gamma_e$ is the coupling parameter between the oscillators, renormalized by relaxation.

The first of these factors is the imaginary part of the FMR susceptibility whose relaxation parameter is modified by the interaction between the oscillators, in accordance with (2.6). When the conditions in (3.6) are satisfied, the second factor in (3.8) approaches unity throughout with the exception of a narrow (as compared with the FMR linewidth) region near $x = 0$. It describes a narrow peak in the inverted, modified, and greatly amplified NMR signal against the broad background of the FMR line (Fig. 3). This phenomenon was first investigated in Ref. 23, where it was called the electron-nuclear magnetic resonance (ENMR). The inversion of the NMR signal is due to the fact that the nuclear oscillator is both excited and detected indirectly through the electron oscillator. Under the FMR conditions, the transverse component $M_\perp$ of the electron magnetization lags in phase by $\pi/2$ behind the radiofrequency field h. The transverse component $\mu_\perp$ of the nuclear magnetization under NMR conditions lags in phase by $\pi/2$ behind the exciting hyperfine field $(-A M_\perp)$. The component $\mu_\perp$ then induces a field $(-A\mu_\perp)$ in the electron system which, in turn, gives rise to an additional term in the transverse component of the electron magnetization m_1, which is in antiphase with $M_\perp$. The result is that the electron signal induced by the nuclear system is in antiphase with the electron system excited by the high-frequency field.

Thus, the phase relationships are found to reconcile the two conditions in (3.6): in accordance with the expressions for the natural frequencies, the two resonance peaks occur at the same point $\omega = \omega_c$, but the linewidths of the modified FMR and modified NMR (Fig. 3) are given in accordance with (2.6) by the expressions

$$\Delta\omega_e = 2\left(\Gamma_e - \frac{\omega_q^2}{4\Gamma_e}\right), \quad \Delta\omega_n = 2\left(\Gamma_n + \frac{\omega_q^2}{4\Gamma_e}\right). \tag{3.9}$$

The relative size of the NMR peak expressed as a fraction of the maximum value of the FMR signal is given by

$$\lambda = \frac{\omega_q^2}{\omega_q^2 + 4\Gamma_e\Gamma_n}. \tag{3.10}$$

The inverted NMR peak becomes greater as $\omega_q^2/4\Gamma_e\Gamma_e$

increases. As $\Gamma_n - 0$, the NMR signal tends to its maximum value, which is equal to the magnitude of the FMR signal. The additional terms in (3.9), i.e., $\omega_q^2/4\Gamma_e$, are negligible in comparison with the FMR linewidth when (3.7) is satisfied, but may be very substantial for NMR.

The ENMR phenomenon (Fig. 3) is thus only outwardly similar to the resonance curves of two coupled circuits with similar damping (Fig. 2); the physical nature of the maxima and minima in Figs. 2 and 3 is quite different.

In further analysis of ENMR, it will be convenient to use a further approximation for the susceptibility of the system. Let us introduce the complex susceptibilities for the unperturbed FMR and NMR

$$\chi_e = \frac{\gamma_e M}{\omega_e - \omega + i\Gamma_e}, \quad \chi_n = \frac{\gamma_n \mu}{\omega_n - \omega + i\Gamma_n}, \tag{3.11}$$

so that the complex susceptibility of the system (3.1) can be written in the form[25]

$$\chi = \frac{\chi_e}{1 - A^2\chi_e\chi_n} \approx \chi_e + (A\chi_e)^2\chi_n. \tag{3.12}$$

The approximate expression on the right-hand side is valid only in the case of a "weak" NMR signal for which $\lambda \ll 1$. It then follows that the imaginary part of the susceptibility is given by

$$\chi'' \approx \chi_e'' + A^2[(\chi_e'^2 - \chi_e''^2)\chi_n'' + 2\chi_e'\chi_e''\chi_n']. \tag{3.13}$$

In contrast to (3.8), this expression is valid for any relationship between the unperturbed frequencies ω_e and ω_n. It is clear that, in the general case, the absorption of energy depends both on the imaginary and real parts of the nuclear and electron susceptibilities. The amplification coefficients for χ_n'' and χ_n' may become imaginary because of the phase relationships in the neighborhood of FMR. It will be more convenient to consider the squares of the coefficients in front of χ_n'' and χ_n':

$$\eta_1^2 = A^2(\chi_e'^2 - \chi_e''^2), \quad \eta_2^2 = 2A^2\chi_e'\chi_e''. \tag{3.14}$$

Let us consider (3.13) and (3.14) in the neighborhood of NMR, for which ω is close to ω_n. The coefficient η_1^2 will tend to the usual expression given by (1.5) when $\omega_n \ll \omega_e$, i.e., it will be determined by the static susceptibility $(A\chi_0)^2$; it will vanish for $|x| = \Gamma_e$ and will become negative within the half-width of the FMR line. The coefficient η_2^2 in front of χ_n' is small in comparison with η_1^2 both near $x = 0$ and for $x \gg \Gamma_e$. It is only on the sloping side of the FMR curve where $x \approx \Gamma_e$ that the contribution of χ_n' to absorption will dominate the contribution due to χ_n''. For $\omega \sim \omega_n$ and different relationships between ω_e and ω_n we have

$$\chi'' \approx \begin{cases} \chi_0\dfrac{\Gamma_e}{\omega_e} + (A\chi_0)^2\chi_n'', & \omega_e \gg \omega_n,\ \Gamma_e, \\ \chi_0\dfrac{\omega_e}{\Gamma_e} - \left(A\chi_0\dfrac{\omega_e}{\Gamma_e}\right)^2\chi_n'', & \omega_e = \omega_n. \end{cases} \tag{3.15}$$

The first of these expressions describes the usual nuclear signal well away from the region of interaction between FMR and NMR, whilst the second expression describes the inverted and amplified nuclear signal in the case of ENMR. The additional amplification of the nuclear signal by the FMR signal is proportional to the square of the ratio of the susceptibility at resonance to the static electron susceptibility, i.e.,

$$K = \left(\frac{\chi_{er}''}{\chi_0}\right)^2. \tag{3.16}$$

We recall that, in practice, we have to use susceptibilities measured in different magnetic fields: χ_{er} in fields corresponding to $\omega_e = \omega_c$ and χ_0 in much stronger fields, for which $\omega_n \ll \omega_e$. This means that K is greater than one would expect from the FMR amplification effect alone.

To be specific, we have confined our attention to ENMR in the simple case of a magnetically isotropic sphere. When anisotropy is introduced in the xy plane, some of the above expressions will become more complicated. Thus, for a thin magnetic film magnetized in its plane at right-angles to the uniaxial anistropy in that plane, the susceptibility of the system is no longer given by (3.1) but by the following expression[23]:

$$\chi = \frac{4\pi(\gamma_e M)^2(\omega_n^2 + 2i\omega\Gamma_n - \omega^2)}{(\omega_e^2 - \omega^2 + 2i\omega\Gamma_e)(\omega_n^2 - \omega^2 + 2i\omega\Gamma_n) - \omega_n^2\omega_q^2}, \tag{3.17}$$

where the parameters of the nuclear system are the same as before but the parameters of the electron system and ω_q are now given by

$$\omega_e = \gamma_e\sqrt{4\pi M(H - H_k)}, \ \Gamma_e = 2\pi\xi\gamma_e M, \quad \omega_q = \gamma_e\sqrt{4\pi A M\mu}. \tag{3.18}$$

However, all the qualitative conclusions remain in force. In addition, all the expressions containing χ_e and χ_n remain valid in their general form given by (3.12)–(3.14) or (3.9)–(3.10) provided, of course, that χ_e, χ_n and the other parameters are suitably redefined.

The absorbed energy of the high-frequency field per unit volume per unit time is given by

$$P = \frac{1}{2}\omega\chi''h^2. \tag{3.19}$$

The form of this function had been analyzed numerically[23] well before the ENMR signal was observed. It was assumed that

$$\omega_n = 4\pi\cdot 10^8\ \text{s}^{-1}, \quad \omega_q = 1.5\cdot 10^8\ \text{s}^{-1}, \quad \Gamma_e = 9\cdot 10^8\ \text{s}^{-1}, \quad \Gamma_n = 5.8\cdot 10^6\ \text{s}^{-1}. \tag{3.20}$$

The value of ω_n corresponds to the NMR frequency in cobalt, where Γ_e was taken from FMR experiments on permalloy films in the microwave band, whilst Γ_n was taken from NMR experiments on single-domain cobalt

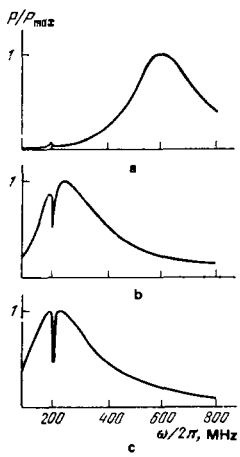

FIG. 4. Absorption of electromagnetic field energy at $\omega_n/2\pi$ = 200 MHz and $\omega_e/2\pi$ = 600 (a), 250 (b), and 200 (c) MHz.

particles. The quantity ω_q corresponds to (3.18) with μ calculated from the Langevin formula for an alloy containing 40% of cobalt at 300°K.

Figure 4 shows the results of these calculations for different values of ω_e and ω_n. It can be seen how the NMR signal (at 200 MHz) is inverted and amplified as the FMR signal "creeps" over it.

C. Shift of FMR

The electron resonance susceptibility is known to be a function of two variables, ω and H, i.e., the resonance can be observed by varying either the frequency or the field. For $\omega_n \ll \omega_e$, the nuclear resonance susceptibility depends on the magnetic field in a nonresonance fashion: NMR can be observed only by varying the frequency. In general, ENMR is a function of two variables, namely, ω and H, but the form of this resonance is qualitatively different when the frequency is varied than when the field is varied. The double-hump ENMR curve was analyzed above in detail. It is obtained by varying the frequency, and we have already considered the kind of information that can be extracted from it. A single-hump curve should be observed when the field is varied (broken curve in Fig. 3). In this section, the ENMR curve is, in fact, FMR modified by the interaction with NMR. The most obvious effect of this modification is clear from Fig. 3 and amounts to a reduction in the resonance FMR susceptibility. The other effect is that the resonance magnetic field is shifted for $\omega \neq \omega_n$. The susceptibility χ'' has a maximum when the field is varied determined by the relation

$$\omega_e = \omega + \left(\frac{\omega_q}{2}\right)^2 \frac{\omega_n - \omega}{(\omega_n - \omega)^2 + \Gamma_n^2}. \tag{3.21}$$

Thus, by investigating the dependence of the FMR resonance field H_0 on frequency near $\omega = \omega_n$, one can determine the real part of the nuclear susceptibility.[25] This is an unexpected result, especially since it does not depend on the relationship between Γ_e, Γ_n, and ω_q, i.e., it is independent of whether or not the natural frequencies separate or cross. In other words, the function $H_0(\omega)$ is unrelated to the behavior of the natural frequencies $\omega'(H)$ (see Fig. 1).

The expression given by (3.21) refers to the isotropic ferromagnetic sphere. In the case of magnetic anisotropy in the x, y plane (shape anisotropy or crystallographic anisotropy), the equation for the resonance field H_0 turns out to be more complicated.[25] For a ferromagnet with $\chi_{0y} \ll \chi_{0x}$,

$$\left[\frac{M}{\chi_{0x}(H_0)} + \tilde{H}_\Delta\right]\frac{M}{\chi_{0y}(H_0)} = \left(\frac{\omega}{\gamma_e}\right)^2; \tag{3.22}$$

and for an antiferromagnet

$$H_0(H_0 + H_D) + H_E\tilde{H}_\Delta = \left(\frac{\omega}{\gamma_e}\right)^2, \tag{3.23}$$

where the effective field $\tilde{H}_\Delta$ describes the effect of the nuclear system on the resonance field H_0:

$$\tilde{H}_\Delta = A^2 M\,[\chi_n^0 - \chi_n'(\omega)]. \tag{3.24}$$

The first term in the last equation describes the longitudinal (static) hyperfine field acting on the electron system, $-A\mu$. The second term is proportional to χ_n' and corresponds to the hyperfine field induced by the transverse components of nuclear magnetization in the electron system. When $\omega \gg \omega_n$, the second term is small and $\tilde{H}_\Delta$ is determined by the static hyperfine field which is readily observed in AFMR because of the exchange amplification.[26] In the overlap region, $\tilde{H}_\Delta$ is determined by the second term, i.e., by the real part of the nuclear susceptibility.

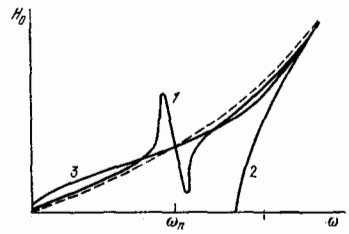

FIG. 5. Curve 1—resonance FMR (AFMR) field H_0 as a function of frequency; curves 2 and 3—natural frequencies for $\Gamma_e \ll \omega_q \ll \omega_n$ and $\omega_q \ll \Gamma_e \ll \omega_n$, respectively. Broken curve corresponds to absence of the nuclear system.[25]

Equations (3.22)–(3.24) are more complicated than (3.21) but, qualitatively, they describe the same effect: as the field is varied ENMR exhibits a single-mode curve representing the modified FMR for which the resonance field H_0 is determined by the real part of the nuclear susceptibility. Figure 5 shows schematically the theoretical[25] dependence of H_0 on frequency (curve 1). For comparison, the figure also shows the natural frequencies of electron-nuclear magnetic oscillations when $\Gamma_e \ll \omega_q \ll \omega_n$ (curve 2) and when $\omega_q \ll \Gamma_e \ll \omega_n$ (curve 3). Similar effects should be observable when FMR and AFMR interact with any other resonance, the frequency of which is independent of the external magnetic field. We note that all the foregoing results are valid only in fields exceeding the saturation field H_s, so that the specimen is in the single-domain state and $\mathbf{M} \parallel \mathbf{H}$. When H_Δ is not high enough, there will be a frequency $\omega > \omega_n$ for which $H_0 = H_s$, i.e., curve 1 in Fig. 5 will "press against" the ω axis.

D. Effect of inhomogeneities

It is well known that the spatial inhomogeneity of the hyperfine field H^n, associated with the inhomogeneity of A and due to different types of defect, is important in NMR and often provides the main contribution to the linewidth and structure of the NMR spectrum of magnetically ordered materials. In general, spatial inhomogeneity of A is very difficult to take into account, and such problems must be solved with the aid of the correlation theory of random functions. Depending on the ratio between the correlation length r_0 of the random function of coordinates $A(r)$ and the correlation length of the exchange interaction, r_α, one can distinguish between two limiting cases, namely, macroinhomogeneity ($r_\alpha \ll r_0$) and microinhomogeneity ($r_0 \ll r_\alpha$). For a uniaxial ferromagnet, for example, the correlation length of the exchange interaction is given by[27]

$$r_\alpha = \sqrt{\frac{\alpha M}{H_k + H}}, \tag{3.25}$$

where $\alpha \sim 10^{-12}$ cm^2 is the exchange interaction constant.

The limiting case of macroinhomogeneity is the sim-

plest. The specimen can be approximately divided into noninteracting pieces with different values of A (since $r_\alpha \ll r_0$). Consequently, one can then introduce a one-dimensional function $f(A)$, which should be used in averaging the susceptibility obtained for one of the members of the ensemble, i.e., a region with constant A. The case of microinhomogeneity is more complicated. Here, the condition is $r_0 \sim a$, where a is the lattice constant, and the macroscopic energy density cannot be written in the form $A\mathbf{M}_\mu$ since the very introduction of $\mathbf{M}$ and μ presupposes averaging over a physically infinitesimal volume of linear size $r_b \gg a$. A different approach must, therefore, be adopted.[28] Let us consider a small but macroscopic volume of radius $r_b \gg r_0$, and let us sum over it by introducing the macroscopic electron magnetization $\mathbf{M}$. The chosen volume will contain a large number of atoms with different values of A. We now divide them into separate groups containing nuclear spins with the same NMR frequency (the same A) although they may be at relatively long distances from each other within the chosen volume of averaging. Each such group of spins, with roughly the same NMR frequency, can be referred to as isochromatic and looked upon as a kind of sublattice. However, in contrast to the antiferromagnet, the number of sublattices is no longer fixed but is determined by the precision with which the isochromatic groups can be identified. By summing over the isochromatic groups, we obtain the nuclear magnetization of the sublattice, μ_k. We neglect direct interaction between the sublattices, and their interaction with the electron magnetization $\mathbf{M}$ (introduced after the summation) is described by the next term in the macroscopic energy density:

$$\mathcal{H}_1 = \mathbf{M} \cdot \sum_{k=1}^{N} A_k \mu_k (A_k), \tag{3.26}$$

where N is the number of isochromatic sublattices. The electron magnetization connected with strong exchange will interact with the resultant field of the nuclear isochromatic groups. It is clear that one can approximately replace summation by integration, so that the final expression for the hyperfine interaction term in the phenomenological Hamiltonian is

$$\mathcal{H}_1 = \mathbf{M} \cdot \int_{-\infty}^{\infty} A\mu (A)\, dA. \tag{3.27}$$

This expression is valid for

$$a \leqslant r_0 \ll r_b \ll r_\alpha, \tag{3.28}$$

where the volume of averaging $\sim r_b^3$ must be large enough to ensure that each sublattice within it contains a sufficiently high number of atoms. This approach is therefore valid only for long-wave oscillations in the electron and nuclear magnetizations: The condition $kr_b \ll 1$ must be satisfied (k is the characteristic wave number) and this is more stringent than that used in the phenomenology of the homogeneous system ($ka \ll 1$).

As in the usual phenomenology, one can use (3.27) at nonzero absolute temperatures much lower than T_c. This presupposes that, in obtaining the magnetization μ_k of a sublattice in (3.26), we did not sum over the sublattice spins but have evaluated the thermodynamic mean. The function $\mu(A)$ is then the magnetization of the sublattice in the field AM at the given temperature T, and can be calculated from the Brillouin formula

$$\mu (A) = Nf (A)\, \gamma_n \hbar I B_I \left(\frac{\gamma_n \hbar I A M}{kT} \right), \tag{3.29}$$

where N is the density of magnetic nuclei and I is the nuclear spin.

The effective magnetic fields corresponding to the interaction $\mathcal{H}_1$ are given by

$$\mathbf{H}_1^e = -\int A\mu (A)\, dA, \quad \mathbf{H}_1^n = -A\mathbf{M}. \tag{3.30}$$

The equations of motion for the system are still given by (1.1) but, now, the Bloch equation describes the motion of the magnetization of one isochromatic sublattice in the field $\mathbf{H}_1^n$, and the Landau-Lifshitz equation describes the motion of the electron magnetization in the resultant field of all the isochromatic sublattices interacting with it.

Thus, the average susceptibility of the electron-nuclear system is given by two different expressions in the two limiting cases[25]: for macroscopic inhomogeneities

$$\chi = \int \frac{\chi_e f (A)\, dA}{1 - (qA)^2 \chi_e \chi_n}, \tag{3.31}$$

and for microscopic inhomogeneities

$$\chi = \frac{\chi_e}{1 - \chi_e \int (qA)^2 \chi_n f (A)\, dA}, \tag{3.32}$$

where $q = 1$ for a ferromagnet and $q = -(2\alpha_e \alpha_n)^{-1}$ for an antiferromagnet; α_e and α_n are the angles between the electron and nuclear sublattices.

In the general case, Eqs. (3.31) and (3.32) are very different. However, for a weak nuclear signal for which λ, as given by (3.10), is small, we can expand the denominators in both formulas into series, and restrict our attention to the leading terms. The two results then become identical. Moreover, the dispersion of q and A is usually small, and their average values q_0 and A_0 can be taken outside the integral sign:

$$\chi \approx \chi_e + (q_0 A_0 \chi_e)^2 \bar{\chi}_n, \quad \bar{\chi}_n = \int \chi_n f (A)\, dA. \tag{3.33}$$

Hence, it is clear that it is the integrated nuclear susceptibility $\bar{\chi}_n$ that appears in the case of the weak nuclear signal both at ENMR and well away from this resonance. If the inhomogeneous broadening of the NMR is small in comparison with the homogeneous broadening, $\bar{\chi}_n$ is not very different from χ_n. When the opposite inequality is satisfied, the integrated nuclear susceptibility is wholly determined by the form of $f(A)$. For example, for alloys, the function $f(A)$ can be a multimode function whose every peak corresponds to a specific atomic species or to the positions of the atoms in the crystal lattice. If we compare (3.33) with (3.12), it is clear that this entire complicated NMR spectrum should be seen in both ENMR planes: It should be seen as the inverted and multiply amplified $\bar{\chi}''(\omega)$ signal along the frequency axis and as a shift of the resonance field, proportional to $\bar{\chi}'(\omega)$, along the field axis.

So far, we have confined our attention to the inhomogeneity of the hyperfine field acting on nuclei. This, however, is not the only type of spatial inhomogeneity that can manifest itself in NMR. Thus, the inhomo-

geneity of the anisotropy field leads to an inhomogeneity in the amplification coefficient η. Naturally, when the conditions for ENMR are satisfied, there are new channels along which the parameters of the electron magnetic system affect the NMR spectrum. This question is only beginning to be investigated. The effect of spatial fluctuations in the anisotropy field on ENMR was investigated in Ref. 25. Such inhomogeneities are known to broaden the FMR line. It turns out that, in the first approximation, these inhomogeneities can also be seen in ENMR as an increase in the effective value of Γ_e. Consequently, the NMR amplification coefficient K in (3.16), which is proportional to $1/\Gamma_e^2$, can be substantially reduced by inhomogeneities in the anisotropy field. On the other hand, the shift of the FMR line, which is proportional to χ_n', has only an indirect effect on the increase in Γ_e (the resonance line is broader, so that the shift in the resonance field is less accurately determined). It follows that, under the conditions of strong inhomogeneity of the anisotropy field, the ENMR signal may turn out to be a more sensitive phenomenon along the magnetic field axis (FMR shift) than along the frequency axis.

E. Experiment

Experimental work in the NMR-FMR overlap region has been carried out on thin metal films containing cobalt nuclei. The specimens were ferromagnetic polycrystals with weak induced uniaxial anisotropy in the plane of the film ($H_k \sim 10$–40 Oe). Such polycrystalline films are usually produced by thermal evaporation in vacuum onto glass or other substrates. The film thickness was $\sim 10^{-5}$ cm, their diameter was ~1 cm, and the magnetization was ~1 000 G. The experiments were performed with both pure cobalt films and alloys of cobalt with iron and nickel. The FMR frequency was reduced to the NMR frequency by an external magnetic field perpendicular to the anisotropy axis [see Eq. (3.18)]. The first attempt to detect effects due to the FMR-NMR overlap was undertaken in 1960.[29] Theoretical papers[10,11] have considered the behavior of the natural frequencies of the system in the neighborhood of the ω_e, ω_n crossing point, and have stimulated further attempts. The first successful experiment was reported in 1971[30] and was concerned with FMR along the field axis at different fixed frequencies. The graph of the resonance field H_0 as a function of frequency (Fig. 6) shows a break in the region where ω_e and ω_n become equal. When the radiofrequency field is increased by a factor of ten, the curve straightens out and the nuclear

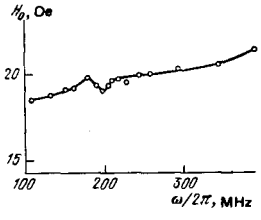

FIG. 6. Measured dependence of the FMR resonance field H_0 on frequency ω.[30] The experiment was performed on a film containing 40% cobalt. FMR was observed by varying the field at fixed frequencies ω.

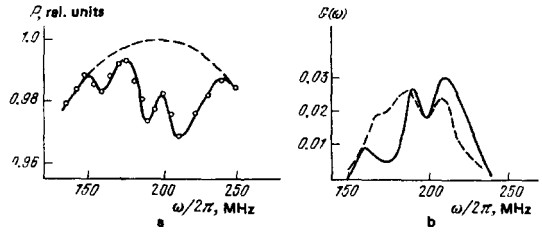

FIG. 7. Experimental graphs obtained at room temperature for an Fe14Ni60Co26 film with a complex NMR spectrum[31]: a—ENMR line ($\Delta = 1\%$; broken curve represents FMR maximum in absence of the nuclear system); b—graph of $G(\omega) = A^2\chi_e(\omega_e/2\Gamma_e)\chi_n''(\omega)$ obtained from curve a (broken line—NMR spectrum of Co^{59}, recorded by the spin echo method with signal/noise ratio = 10; ordinate scale is the same as for the $G(\omega)$ graph). Here and below the figure captions contain an indication of the relative measurement error Δ.

magnetization saturation effect decouples the nuclear system from the electron system. It was concluded[30] that this experiment yielded the natural frequencies of the system modified by relaxation, i.e., curve 3 of Fig. 5. The experiment stimulated further theoretical work[13] in which the frequencies of electron-nuclear oscillations were investigated for the first time with allowance for damping. Qualitatively, the shape of the $\omega'(H)$ curve for electron-like oscillations turned out to be close to that shown in Fig. 6, but the observed FMR shift differed from the theoretical prediction by an order of magnitude. The reason for this discrepancy remained unclear until it was shown[25] that the function $H_0(\omega)$ plotted along the field axis described χ_n' (curve 1 in Fig. 5) and had no relation to the $\omega'(H)$ curve.

ENMR was demonstrated experimentally for the first time in 1975[31] along the frequency axis, soon after it was predicted theoretically.[23] The solid curve in Fig. 7a shows the ENMR spectrum recorded for an Fe14Ni60Co26 film at room temperature. The broken curve in Fig. 7a is the top of the FMR line in the absence of the nuclear signal. The NMR signal amplified by FMR should be measured from this curve in the downward direction. Since the NMR spectrum of this film is relatively broad, analysis of the ENMR signal must take into account the variation in the amplification coefficient η, given by (3.14), across the FMR line. The susceptibility χ_n'' of the nuclear system deduced from Fig. 7a is shown in Fig. 7b (solid line). The broken line in this figure shows (on an arbitrary scale) the NMR signal recorded for the same film by the spin echo method well away from the region of overlap of the resonance frequencies. It is clear that the spectrum structure is very similar. Figure 8 shows similar measurements and analyses of the ENMR signal at liquid nitrogen temperatures.[32] As can be seen, there is a sharp rise in the nuclear susceptibility: the NMR signal now amounts to 20% of the FMR signal. The additional amplification K of the nuclear signal in ENMR, compared with the signal observed without the imposition of the external magnetic field, as given by (3.16), was found to reach $K = 300$ at liquid nitrogen temperatures. The substantial amplification of the signal in ENMR has suggested[31,32] the use of very simple equipment, i.e., slightly modernized standard Q-meters

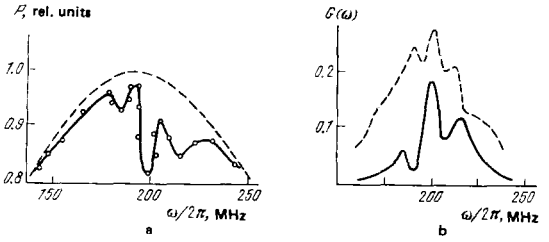

FIG. 8. Experimental graphs for Fe14Ni60Co26 film at liquid nitrogen temperatures[32]: a—ENMR line ($\Delta = 3\%$); b—graph of $G(\omega)$ and the NMR spectrum of Co^{59} with signal/noise ratio = 20. Notation the same as in Fig. 7.

(type E9-5).

Recently, ENMR has also been investigated experimentally[25] along both the frequency and the field axes. The observations were performed with a combined apparatus (Fig. 9) capable of measuring active losses in the specimen and observing the spin echo. The spin-echo signal from the probe D was amplified in the receiving channel R and was recorded by the oscillograph CRO. A continuous oscillator O_c was connected to the probe used to record ENMR. In the case of the experiments along the frequency axis, the absorption of energy P_1 in the specimen at overlap ($\omega_e = \omega_n$ and $\mathbf{H} \perp \mathbf{h}$) was compared with the absorption P_0 in a strong field $\mathbf{H} \parallel \mathbf{h}$ where it was practically independent of frequency. The measurements were therefore expressed in relative units: $P(\omega) = P_1(\omega)/P_0$. Figure 10 shows the experimental graphs for the specimen with a single-peak NMR spectrum. It is clear that the $\chi_n'(\omega)$ and $\chi_n''(\omega)$ curves are in satisfactory agreement with one another. The possibility of simultaneous measurements of $\chi_n'(\omega)$ and $\chi_n''(\omega)$ improve the reliability of these results very considerably. Experiments have also been performed on the same specimens at liquid helium temperatures.[33] The FMR signal $P(H)$ was observed in these experiments only at frequencies ω exceeding a critical value. It would appear that this effect is connected with the large magnitude of $\tilde{H}_\Delta$ [see Eq. (3.22)]. Whenever the nuclear system was saturated, the FMR signal was observed at any frequency.

4. TRANSIENT PROCESSES

A. Nuclear-electron relaxation and spin echo

Transient processes in the region of overlap between the nuclear and electron resonances should be exceedingly varied. If the natural frequencies of electron-nuclear oscillations are split ($\omega_q > \Gamma_e$), the leading features of the transient phenomena are probably deter-

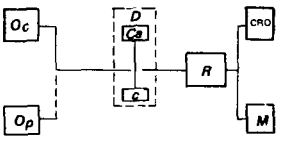

FIG. 9. Block diagram of apparatus:[25] O_c—continuous oscillator; O_p—pulsed oscillator; D—detector; Ca—capacitor, C—coil containing specimen; R—receiver, CRO—oscillograph; M—meter.

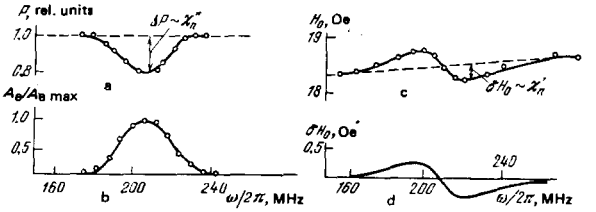

FIG. 10. Experimental graphs obtained for an Fe9Ni21Co70 film with a simple single-peak NMR spectrum at liquid nitrogen temperatures[25]: a—ENMR line ($\Delta = 3\%$; broken curve represents top of FMR line in absence of the nuclear system; on the scale of the figure, the latter is practically a straight line); b—NMR spectrum of Co^{59}, recorded by the spin echo method with signal/noise ratio = 20; c—FMR resonance field H_0 as a function of frequency ω ($\Delta = 0.5\%$); broken line represents the graph in absence of the nuclear system; d—shift of the FMR resonance field, $\delta H_0 \sim \chi_n'(\omega)$, as a function of frequency ω.

O_c

mined by the dynamic frequency shift. One would expect that some of them would be analogous to the phenomena observed well away from the overlap region under the conditions of strong dynamic frequency shift.[6-8] If the natural frequencies overlap ($\omega_q < \Gamma_e$), the situation is more complicated because $D = 0$ at the crossing point and the electron magnetization $\mathbf{M}$ may, generally speaking, undergo nutation with frequency $\gamma_e h$ under the influence of the resonant hf field $\mathbf{h}$. It is only in the limiting case where the electron relaxation parameter Γ_e is much greater than all the characteristic parameters representing the motion of the nuclear magnetization that the theoretical analysis becomes much simpler.[15] One can then neglect transient processes in the electron system and consider the transient phenomena in the nuclear system separately. The main feature of such phenomena is the sharp increase in the nuclear electron relaxation which has already been mentioned in Section 2. It is clear that, if the shift D well away from the overlap point exceeds the NMR linewidth, the characteristic NMR time $T_\varkappa = 1/\Gamma_\varkappa$ at $\omega_e = \omega_n$ will be the shortest relaxation time in the nuclear system, since $\max \Gamma_\varkappa = 2 \max D$. It is readily shown that, if NMR provides the main contribution to nuclear relaxation, the relaxation process will proceed with constant modulus of nuclear magnetization $|\mu|$. Naturally, it will not then be possible to observe the spin echo. If we neglect transient processes in the electron system, we can consider the nonlinear equations of motion for the nuclear magnetization, such as those given by (1.10), just as in the case of points well removed from the overlap region. Instead of (1.9), we then obtain the following expression for the resonance components of the circular projections:

$$m^+ = \chi_e (h^+ - A\mu^+); \tag{4.1}$$

where χ_e is the complex electron susceptibility, i.e., in contrast to the case where $\omega_n \ll \omega_e$, we take into account the fact that the electron magnetization $\mathbf{M}_\perp$ lags in phase behind the effective field acting upon it. The nonlinear terms in (1.10) then become

$$\begin{aligned} L_x &= -Dmu + \Gamma_\varkappa mv, \\ L_y &= Dmv + \Gamma_\varkappa mu, \end{aligned} \tag{4.2}$$

i.e., we have the additional term describing NMR. We note that the amplification coefficient for the hf field

and the nuclear signal in pulsed experiments is given by

$$\eta = A \mid \chi_e \mid_{\omega=\omega_n}, \tag{4.3}$$

i.e., it is determined by the modulus of the electron susceptibility and rises sharply as $\omega_e(H) - \omega_n$. In contrast to the stationary method, the phase relationships between h, **M**, and μ play no role in this case. In the absence of this high-frequency field, the equations of motion for the nuclear magnetization (1.10), taking (4.2) into account, will describe NER. If we neglect the weak dependence of χ_e on μ_z, we can readily integrate these equations[15] and obtain

$$\operatorname{tg}\frac{\theta(t)}{2} = \exp(-\Gamma_\varkappa t)\operatorname{tg}\frac{\theta_0}{2}; \tag{4.4}$$

where $\theta(t)$ is the angle by which μ deviates from its equilibrium position and θ_0 is the initial deviation of μ. It is clear that only the angle between **M** and μ will vary during the NER process. We also note that, if the NER mechanism dominates the situation, the decay of free precession will be replaced by a radiation burst for $\theta_0 > \pi/2$. It must be remembered that, when $\theta_0 > \pi/2$, another process is possible in principle, namely, spontaneous growth of nuclear-like spin waves.[15,16] This process is most probable for θ_0 approaching π, so that the initial amplitude of homogeneous deviation is small. In this situation, the frequencies of nuclear-like spin waves are given by (2.23) provided we introduce the replacement $\mu \to (-\mu)$. It is clear that, when $\Gamma_{\varkappa k} > \Gamma_n$, the nuclear-like wave will grow and will not be damped. If, at the same time, $\Gamma_{\varkappa k} > \Gamma_\varkappa$, the homogeneous transient process will not be possibility because of the decay of nuclear magnetization into nuclear-like spin waves.

We must now consider the case where the time for reversible dephasing of nuclear spins due to the inhomogeneity of the hyperfine field is less than the NER time ($1/\Gamma_3 = T_3 < T_\varkappa$). (This corresponds to the case of weak nuclear signals in the stationary method.) If the inhomogeneity of the field acting on the nuclei is macroscopic, the specimen can be divided into quasi-noninteracting regions, in each of which the field is homogeneous (see Sec. 3). In each such region, the magnetization will return to its equilibrium state $\theta = 0$ in a time $\sim T_\varkappa$. The nuclear spin echo will therefore be observable only for time $t \lesssim T_\varkappa$. The situation is quite different when the inhomogeneity of the hyperfine field is microscopic. The nonlinear terms in (1.10) then assume the form[28]

$$\left.\begin{aligned} L_x &= -DmK_u + \Gamma_\varkappa m K_v, \quad L_y = DmK_v + \Gamma_\varkappa m K_u, \\ L_z &= D(vK_u - uK_v) - \Gamma_\varkappa(uK_u + vK_v), \\ K_u &= \int uf(A)\,dA, \quad K_v = \int vf(A)\,dA. \end{aligned}\right\} \tag{4.5}$$

In this case, the electron magnetization interacts with the resultant field of the nuclear isochromatic group so that nonlinear effects are "turned on" only during the intermediate times for which the nuclear spins are in phase and $\mu_\perp \neq 0$. Consequently, NER is effective only during the short intermediate times corresponding to the decay of free precession and the evolution of spin echo. In other words, microscopic inhomogeneity suppresses NER, but this suppression has nothing in common with the well-known[34-37] suppression of transverse relaxation T_2.

In fact, $\Gamma_\varkappa$ does not change, and the effect is due to the fact that the time Δt during which NER is operative in pulsed experiments is very short: $\Delta\tau \sim T_3$. The relative change in the amplitude of the nuclear spin echo due to NER is of the order of $\Gamma_\varkappa T_3$.[28]

B. ENMR in inverted state

Let us now consider quasistationary transient processes. Suppose that, at the initial time $t = 0$, the nuclear magnetization is in the inverted state $\mu_z = \mu$. For narrow NMR lines, inversion can be produced by a high-frequency π pulse, or, for a system with a broad NMR spectrum, by a remagnetizing pulse applied to the electron system.[16,38] When $t > 0$, the nuclear magnetization relaxes slowly with characteristic time T_1:

$$\mu_z = \mu(2e^{-t/T_1} - 1). \tag{4.6}$$

If, at the same time, a sufficiently weak high-frequency field is applied to the system, the transverse component of μ will "rock" only slightly, and the longitudinal component will, as before, relax in accordance with (4.6). In magnetically unordered systems in the inverted state, the energy of the hf field will be amplified rather than absorbed. Such effects have already been observed experimentally (see, for example, Refs. 39 and 40). The well-known first experiment in this field[39] recorded stimulated coherent emission. In magnetic materials, the situation is complicated by the fact that NMR is always observed against the background of nonresonant electron absorption. Moreover, as already noted, NMR is itself in fact an electron signal induced by the nuclear system. Theoretical calculations[41] have shown that the amplification of the energy of the resonance hf field by the inverted nuclear system of a ferromagnet well away from the NMR-FMR overlap region is possible only when the additional condition $\omega_q^2/4\Gamma_e\Gamma_n > 1$ is satisfied. When this is so, the NMR amplitude will exceed nonresonant electron absorption.

When the NMR and FMR frequencies are equal, quasistationary transient processes can be observed only when nuclear-like oscillations (and nuclear-like spin waves) are damped in the inverted state ($\mu_z = \mu$) in a time much shorter than the longitudinal relaxation time:

$$\omega_n, \ \omega_{nk} \gg \frac{1}{T_1}. \tag{4.7}$$

If the natural oscillations of $\mu_\perp$ are damped, the quasistationary process in the overlap region will occur as for $\omega_n \ll \omega_e$: the projection μ_z of nuclear magnetization will relax with characteristic time T_1, and $\mu_\perp$ will "rock" slightly under the influence of the weak hf field. The ENMR line in the inverted state has the inverted shape as compared with the normal state: a narrow peak representing the additional nuclear absorption (shown broken in Fig. 11) appears against the background of the broad electron resonance maximum. As μ_z relaxes, the amplitude of this peak decreases, and the peak vanishes altogether when $\mu_z = 0$. The inverted signal then appears and gradually approaches its stationary level (solid curve in Fig. 11). We note that,

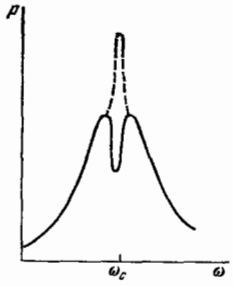

FIG. 11. ENMR spectrum in the normal state (solid curve) and in the inverted state (broken curve).

when the inhomogeneity of the hyperfine field is microscopic, the sufficient condition for the realization of the quasistationary process is $T_3 \ll T_1$, since the dynamic hyperfine interaction will be effective only during the time $\sim T_3$.

Let us now consider one further interesting situation. As already noted in Sec. 2, the minimum frequency of the electron spin wave, ω_{ek}^{min}, may turn out be lower (or even much lower) than the frequency ω_e of the homogeneous resonance. It follows that the frequencies of an entire group of electron spin waves can be made equal to the NMR frequency by applying a suitable magnetic field H and, at the same time, ensuring that $\omega_n \ll \omega_e(H)$. If, in this situation, the nuclear magnetization is inverted ($\mu_z = \mu$), we have the possibility of spontaneous growth of nuclear-like spin waves. The theoretical analysis reported in Ref. 42 appears to be applicable to this situation if we suppose that the main contribution to the relaxation of the z component of nuclear magnetization is due to one-magnon processes: inversion of the nuclear spin is accompanied by the creation of a resonance magnon with $\omega_{ek} = \omega_n$. It turns out that this may give rise to the "magnon bottleneck:" the energy of the excited nuclear spins is transferred to the system of resonance magnons with other degrees of freedom. The system of resonance magnons is therefore overheated, and becomes essentially a nonequilibrium system. The necessary condition for this bottleneck is that $\sigma \gg 1$, where σ is the dimensionless bottleneck parameter. To within a factor of $\sqrt{3}$, the parameter σ for ferro- and antiferromagnets is given by the same expression[42]: $\sigma = (D/\Gamma_n^*)(\omega_e/\Gamma_{ek})$, where Γ_{ek} is the damping parameter for the resonance magnons and Γ_n^* is the effective NMR line half-width. When $D \ll \Gamma_n^*$, but $\omega_e \gg \Gamma_{ek}$ and $\sigma \gg 1$, the dynamic frequency shift is practically zero, and the main features of transient processes may be connected with the magnon bottleneck. When the bottleneck occurs for $\mu_z > 0$, the rate of relaxation of μ_z will be initially greater than for $\mu_z < 0$, and this will, of course, have an effect on pulsed experiments. Similar effects have already been observed in electron-type paramagnetics under the conditions of the phonon bottleneck.[43]

C. Experiment

We must now examine the results of experimental studies of transient processes in the region of the ω_e, ω_n overlap. Pulsed experiments have been performed with the same specimens and under the same conditions as in stationary experiments. The nuclear spin echo was reliably observed in the NMR, FMR overlap region

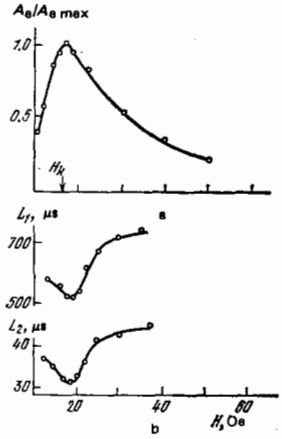

FIG. 12. Experimental graphs obtained for the specimen shown in Fig. 10[15]: a—spin echo amplitude A_e as a function of external magnetic field H with signal/noise ratio not less than 10; b—L_1 and L_2 as functions of H ($\Delta = 5\%$).

and the delay time between pulses was usually much greater than the characteristic NER time T_w. This means that the inhomogeneity of the hyperfine field in these specimens was microscopic. The spin-echo amplitude always rises sharply as $\omega_e \to \omega_n$ (Fig. 12a). Hence, it is clear that, when pulsed methods are employed, weak nuclear signals are again more conveniently investigated in the NMR, FMR overlap region. It has been shown[44] that, in the overlap region, the amplitude of the three-pulse stimulated echo, A_e^{st}, decreases with increasing delay τ_{23} between the second and third pulses two or three times more rapidly than well away from the overlap region. [When $\omega_n \ll \omega_e(H)$, the function $A_e^{st}(\tau_{23})$ is determined by T_1.] It has been suggested that this effect could be used in radioengineering.[45] Figure 12b shows graphs obtained by the two-pulse echo method[25] with the same specimen as in Fig. 10. The dependence of the echo amplitude A_e on the delay time τ is approximately represented by an exponential with characteristic time L_2 ($L_2 = T_2$ for $\omega_n \ll \omega_e$). Figure 12b shows that there is a substantial reduction in L_2 in the overlap region. Other experiments have also been performed with this specimen. A preliminary pulse was used to excite the nuclear system, and then the usual spin-echo program was turned on after a time τ_0. The dependence of the echo amplitude on τ_0 was again represented approximately by an exponential with a characteristic time L_1 ($L_1 = T_1$ for $\omega_n \ll \omega_e$). It is interesting that the relative changes in L_1 and L_2 in the overlap regions are the same although the absolute magnitude of L_1 is greater by an order of magnitude than that of L_2. It has been suggested[25] that the reduction in L_1 and L_2 in the overlap region is connected with the NER mechanism.

The first report of an experimental demonstration of the nuclear spin echo in the NMR, FMR overlap region at helium temperatures has recently been published.[33]

CONCLUSIONS

It is clear from our brief review that the region of overlap between the nuclear and electron resonances

is no longer an exotic speculation indulged in by theoretical physicists. The discovery of new phenomena such as ENMR and the FMR shift that is proportional to the real part of the nuclear susceptibility, which have been confirmed experimentally, shows that this new branch of the science of magnetic resonance has very attractive possibilities. Experiments performed in the region in which the resonances overlap will help the development of research into the properties of other physical systems and will open up new possibilities for the spectroscopy of magnetic materials. The strong dependence of the nature of the transient processes in the NMR, FMR overlap region on the inhomogeneity correlation length can be used to investigate the properties of new promising amorphous magnetic materials. Effects such as amplification of the nuclear spin-echo signal, acceleration of relaxation, and ENMR are very likely to find applications in high-frequency devices. It is important to note, however, that, so far, the experiments have been confined to polycrystalline cobalt-permalloy films and, as a rule, nitrogen or room temperatures, i.e., conditions corresponding to a "weak" nuclear signal. Nonlinear effects (including NER), saturation effects, and quasistationary processes remain practically uninvestigated. Experimental difficulties are connected, in the first instance, with the necessity for lowering the electron resonance frequency down to the NMR value in such a way that a domain structure does not appear. However, the value of the information that can be extracted from experiments in the region of strong ineraction between FMR and NMR should serve as a stimulus for efforts to overcome these difficulties.

[1]L. D. Landau and E. M. Lifshitz, Phys. Z. Sowjetunion 8, 153 (1935).
[2]F. Bloch, Phys. Rev. 70, 460 (1946).
[3]E. A. Turov and M. P. Petrov, Yadernyĭ magnitnyĭ rezonans v ferro- i antiferromagnetikakh (Nuclear Magnetic Resonance in Ferro- and Antiferromagnets), Nauka, M., 1969.
[4]A. Narat, in: Hyperfine Interactions in Solids (Russian translation, Mir., M., 1969).
[5]W. Zinn, Atom. Energ. Rev. 12, 709 (1974).
[6]E. A. Turov and M. I. Kurkin, V. kn Problemy magnitnogo rezonansa (in: Problems of Magnetic Resonance), Nauka, M., 1978, p. 271.
[7]M. P. Petrov, V. P. Chekmarev, and A. P. Paugurt, *ibid.*, p. 289.
[8]Yu. M. Bun'kov and B. S. Dumesh, *ibid.*, p. 310.
[9]E. A. Turov, M. I, Kurkin, and V. V. Nikolaev, Zh. Eksp. Teor. Fiz. 64, 283 (1973) [Sov. Phys. JETP 37, 147 (1973)].
[10]V. A. Ignatchenko and Yu. A. Kudenko, Izv. Akad. Nauk SSSR Ser. Fiz. 30, 77 (1966); v kn. Radiospektroskopiya tverdogo tela (in: Radiospectroscopy of Solids), Atomizdat, M., 1967, p. 181.
[11]L. G. Onoprienko, Fiz. Met. Matalloved. 19, 481 (1965).
[12]E. Z. Turov and V. G. Kuleev, Zh. Eksp. Teor. Fiz. 49, 248 (1965) [Sov. Phys. JETP 22, 176 (1966)].
[13]A. M. Portis, AIP Conf. Proc. (USA) 10, Pt. 1, 120 (1972).
[14]V. A. Ignatchenko and V. I. Tsifrinovich, Preprint IFSO-29F, Krasnoyarsk, 1975.
[15]V. I. Tsifrinovich and V. A. Ignatchenko, Zh. Eksp. Teor. Fiz. 72, 803 (1977) [Sov. Phys. JETP 45, 419 (1977)].
[16]V. A. Ignatchenko and Yu. A. Kudenko, Izv. Akad. Nauk SSSR Ser. Fiz. 30, 933 (1966).
[17]D. Sherrington, J. Phys. C 3, 2359 (1970); 4, 625 (1971).
[18]M. G. Gottam and M. J. Jones, *ibid.* 6, 1020 (1973).
[19]J. W. Tucker, Phys. Status Solidi B 60, 271 (1973).
[20]A. I. Akhiezer, V. G. Bar'yakhtar, and S. V. Peletminskiĭ, Spinovye volny (Spin Waves), Nauka, M.,(1967) (published in English by North-Holland, Amsterdam).
[21]V. V. Migulin, V. I. Medvedev, E. R. Mustel', and V. N. Parygin, Osnovy teorii kolebaniĭ (Fundamentals of the Theory of Oscillations), Nauka, M., 1978.
[22]M. N. Botvinko and M. A. Ivanov, Fiz. Terd. Tela (Leningrad) 15, 1704 (1973) [Sov. Phys. Solid State 15, 1142 (1973)].
[23]V. A. Ignatchenko and V. I. Tsifrinovich, Zh. Eksp. Teor. Fiz. 68, 672 (1975) [Sov. Phys. JETP 41, 333 (1975)].
[24]V. A. Ignatchenko, Yu. A. Kudenko, V. I. Tsifrinovich, I. A. Lyapunov, K. V. Mal'tsev, and N. M. Salanskiĭ, V kn Fundamental'nye issledovaniya: Fiziko-matematicheskie i tekhnicheskie nauki (in: Fundamental Studies: Physico-mathemmathical and Technical Sciences), Nauka, Novosibirsk, 1977, p. 218.
[25]V. A. Ignatchenko, V. K. Mal'tsev, and V. I. Tsifrinovich, Zh. Eksp. Teor. Fiz. 75, 217 (1978) [Sov. Phys. JETP 48, 108 (1978)].
[26]A. S. Borovik-Romanov, V. kn. Problemy magnetizma (in: Problems in Magnetism), Nauka, M., 1972, p. 47.
[27]V. A. Ignatchenko, Zh. Eksp. Teor. Fiz. 54, 303 (1968) [Sov. Phys. JETP 22, 162 (1968)].
[28]V. I. Tsifrinovich, Fiz. Tverd. Tela (Leningrad) 20, 1657 (1978) [Sov. Phys. Solid State 20, 959 (1978)].
[29]P. E. Tannenwald and E. Walters, Quarterly Progress Report Solid State Res. Lincoln Lab. Mass. Inst. Technol., July 1960; October, 1960.
[30]A. N. Pogorelyĭ and V. V. Kotov, Pis'ma Zh. Eksp. Teor. Fiz. 14, 305 (1971) [JETP Lett. 14, 202 (1971)].
[31]V. A. Ignatchenko, N. M. Salanskiĭ, V. K. Mal'tsev, and V. I. Tsifrinovich, *ibid.* 21, 472 (1975) [JETP Lett. 21, 218 (1975)].
[32]V. A. Ignatchenko, V. K. Mal'tsev, and V. I. Tsifrinovich, Fiz. Tverd. Tela (Leningrad) 19, 2036 (1977) [Sov. Phys. Solid State 19, 1191 (1977)].
[33]V. V. Kotov and A. N. Pogorelyĭ, Pis'ma Zh. Eksp. Teor. Fiz. 28, 621 (1978) [JETP Lett. 28, 574 (1978)].
[34]D. Hone, V. Jaccarino, T. Ngwe, and P. Pincus, Phys. Rev. 186, 219 (1969).
[35]M. I. Kurkin and V. V. Serkov, Fiz. Tverd. Tela (Leningrad) 12, 3524 (1970) [Sov. Phys. Solid State 12, 2862 (1971)].
[36]J. Barak, I. Siegelstein, A. Gabai, and N. Kaplan, Phys. Rev. B 8, 5282 (1973).
[37]E. D. Shaw, *ibid.* 2, 2746 (1970).
[38]N. M. Salanskiĭ, I. A. Lyapunov, and V. K. Mal'tsev, Pis'ma Zh. Eksp. Teor. Fiz. 13, 694 (1971) (JETP Lett. 13, 491 (1971)].
[39]E. M. Purcell and R. V. Pound, Phys. Rev. 81, 279 (1951).
[40]M. V. Kondrat'ev, M. A. Korchenkin, and Khabibullin, V kn. 19-e Vsesoyuznoe soveshchanie po fizike sizkikh temperatur: Tezisy (in: Nineteenth All-Union Conf. on Low-Temperature Physics: Abstracts), Minski, 1976, p. 680.
[41]V. A. Ignatchenko and V. I. Tsifrinovich, Zh. Eksp. Teor. Fiz. 69, 1243 (1975) [Sov. Phys. JETP 42, 635 (1975)].
[42]S. V. Ivanov, E. A. Turov, and M. I. Kurkin, Fiz. Tverd. Tela. (Leningrad) 18, 2038 (1976) [Sov. Phys. Solid State 18, 1186 (1976)]; 18, 3304 (1976) [Sov. Phys. Solid State 18, 1925 (1976)].
[43]A. Abragam and B. Bleaney, Electron Paramagnetic Resonance of Transition Ions, Oxford University Press, 1970 (Russ. transl., Mir, M., 1972).
[44]S. P. Repnikov and V. B. Ustinov, Fiz. Tverd. Tela (Leningrad) 11, 499 (1969) [Sov. Phys. Solid State 11, 395 (1969)].
[45]V. B. Ustinov and S. P. Repnikov, Soviet Patent 229596, Byull. Izobret. Tov. Znakov, 33 (1968).

Translated by S. Chomet